Multimedia Systems 7: 119–128 (1999)

Multimedia Systems

A feature-based algorithm for detecting and classifying production effects

Ramin Zabih, Justin Miller, Kevin Mai

Computer Science Department, Cornell University, Ithaca, NY 14853, USA; e-mail:rdz@cs.cornell.edu

Abstract. We describe a new approach to the detection and classification of production effects in video sequences. Our method can detect and classify a variety of effects, including cuts, fades, dissolves, wipes and captions, even in sequences involving significant motion. We detect the appearance of intensity edges that are distant from edges in the previous frame. A global motion computation is used to handle camera or object motion. The algorithm we propose withstands JPEG and MPEG artifacts, even at high compression rates. Experimental evidence demonstrates that our method can detect and classify production effects that are difficult to detect with previous approaches.

Key words: Content-based indexing and retrieval – Scene break detection

1 Introduction

The amount of digital video that is available has increased dramatically in the last few years, but the tools available for browsing video remain quite primitive. Computer vision techniques can support content-based browsing of image sequences. For example, we may be able to replace the "fast forward" button on current video browsers with a button that searches for the next dissolve. This will require algorithms to automatically detect such events. This paper presents an algorithm for detecting and classifying production effects (including cuts, fades, dissolves, wipes and captions) in digital video sequences.

The most common production effects are scene breaks, which mark the transition from one sequence of consecutive images (or scene) to another. A cut is an instantaneous transition from one scene to the next. A fade is a gradual transition between a scene and a constant image (*fade-out*) or between a constant image and a scene (*fade-in*). During a fade, images have their intensities multiplied by some value α. During a fade-in, α increases from 0 to 1, while during a fade-out α decreases from 1 to 0. The speed with which α changes controls the fade rate. A dissolve is a gradual transition from one scene to another, in which the first scene fades out and the second scene fades in. Typically, fade-out and fade-in begin at the same time, and the fade rate is constant. Another common scene break is a wipe, in which a line moves across the screen, with the new scene appearing behind the line.

The detection and classification of scene breaks is a first step in the automatic annotation of digital video sequences. The problem is also important for other applications, including compression and automatic keyframing. Motion-based compression algorithms like MPEG can obtain higher compression rates without sacrificing quality when the locations of scene breaks are known. Knowledge about scene breaks can be used to look for higher level structures (such as a sequence of cuts between cameras), or to ensure that keyframes come from different scenes.

We begin with a survey of related work on scene break detection. These methods rely directly on intensity data, and have difficulty with dissolves and with scenes involving motion. We then present our feature-based approach to the problem, which detects the appearance of new edges far from old ones. We show that our methods robustly tolerate compression artifacts. We then present an empirical evaluation of our method, on 50 randomly selected MPEG movies containing scene breaks. We have found no cases where our method fails but where intensity-based methods succeed. Finally, we discuss some of the current limitations of our algorithm and describe extensions which we hope will overcome them.

1.1 Existing algorithms for detecting scene breaks

Scene breaks are detected by computing and thresholding a similarity measure between consecutive images. Existing work has relied directly on intensity data, using such techniques as image differencing and intensity histogramming. Most approaches are based on intensity histograms, and concentrate on cuts [7, 8] These methods have difficulty with "busy" scenes, in which intensities change substantially from frame to frame. Such changes often result from camera or object motion.

Cuts usually result in a dramatic change in image intensities, so they can be detected much of the time. However, a dissolve is a gradual change of all the intensities,

Correspondence to: R. Zabih

and cannot be easily distinguished from motion. A dissolve can even occur between two scenes each containing motion. Thus, dissolves are more difficult to detect than cuts, especially if the scenes involve motion. Increasing the detection threshold can reduce false positives due to motion, but at the risk of missing gradual scene transitions.

Hampapur et al. [4] use an explicit model of the video production process to detect a variety of scene breaks. While their approach is intensity-based, it does not involve histogramming. Instead, they compute a chromatic image from a pair of consecutive images. Its value at each pixel is the change in intensity between the two images divided by the intensity in the later image. Ideally, the chromatic image should be uniform and non-zero during a fade.

The difficulties caused by motion and by dissolves are well-known. For example, Hampapur et al. note in their discussion of dissolves that their measure "is applicable if the change due to the editing dominates the change due to motion"[4, page 11], and describe both object and camera motion as causes of false positives for their method. Another recent paper [11] describes motion as a major limitation of histogram-based methods. The only published comparative analysis of scene break detection methods, due to Boreczky and Rowe [1], concludes that existing methods "do a poor job of identifying gradual transitions".

Zhang et al. [11] have extended conventional histogram-based approaches to handle dissolves and to deal with certain camera motions. They use a dual threshold on the change in the intensity histogram to detect dissolves. In addition, they have a method for avoiding the false positives that result from certain classes of camera motion, such as pans and zooms. They propose to detect such camera motion and suppress the output of their scene break measure during camera motion.

Their method does not handle false positives that arise from more complex camera motions or from object motion. Nor does their method handle false negatives that occur in dissolves between scenes involving motion. In Sect. 4, we will provide an empirical comparison of our method with histogram-based techniques and with chromatic scaling.

2 A feature-based approach

Our approach is based on a simple observation: during a cut or a dissolve, new intensity edges appear far from the locations of old edges. Similarly, old edges disappear far from the location of new edges. We define an edge pixel that appears far from an existing edge pixel as an *entering* edge pixel, and an edge pixel that disappears far from an existing edge pixel as an *exiting* edge pixel. By counting the entering and exiting edge pixels, we can detect and classify cuts, fades and dissolves. By analyzing the spatial distribution of entering and exiting edge pixels, we can detect and classify wipes.

The algorithm we propose takes as input two consecutive images I and I'. We first perform an edge detection step, resulting in two binary images E and E'. Let ρ_{in} denote the fraction of edge pixels in E' which are more than a fixed distance r from the closest edge pixel in E. ρ_{in} measures the proportion of entering edge pixels. It should assume a high value during a fade-in, or a cut, or at the end of a dissolve.[1]

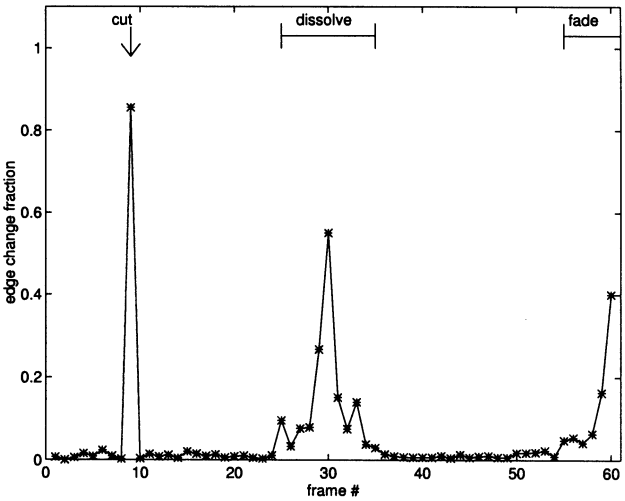

Fig. 1. Results from the table tennis sequence

Similarly, let ρ_{out} be the fraction of edge pixels in E which are farther than r away from the closest edge pixel in E'. ρ_{out} measures the proportion of exiting edge pixels. It should assume a high value during a fade-out, or a cut, or at the beginning of a dissolve.

Our basic measure of dissimilarity is

$$\rho = \max(\rho_{in}, \rho_{out}) . \tag{1}$$

This represents the fraction of changed edges; this fraction of the edges have entered or exited. Scene breaks can be detected by looking for peaks in ρ, which we term the *edge change fraction.*

An example of the edge change fraction is shown in Fig. 1. The sequence we have chosen is the widely known "table tennis" sequence, which was used to benchmark MPEG implementations. The original sequence contains a fair amount of motion (including zooms), plus a few cuts. To demonstrate our algorithm, we have spliced together several parts of the sequence and inserted a few scene breaks. The modified table tennis sequence contains a cut (taken from the original sequence) between frames #9–#10. We have added a dissolve in frames #25–#35, and then a fade-out starting at frame #55. On this sequence, ρ shows clear peaks at the scene breaks, and the detection and the classification algorithm described in Sect. 3.1 performed correctly.

2.1 Motion compensation

Our method can be easily extended in order to handle motion. We can use any registration technique [2] to compute a global motion between frames. We can then apply this global motion to align the frames before detecting entering or exiting edge pixels. For example, assume that the camera is moving to the left, and so image I' is shifted to the right with respect to image I. A registration algorithm will compute the translation that best aligns I with I' (which in this

[1] Due to the quantization of intensities, new edges will generally not show up until the end of the dissolve.

example is a shift to the right). We can apply this translation to I before computing the edge change fraction as shown above.

There are a wide variety of registration algorithms reported in the literature. The ones we have used involve global similarity measures between images, and are based on correlation. Note that we only search for a translational motion between the two images. While it is possible to handle affine or projective motions, they incur significant additional overhead, and do not necessarily result in better performance. We can then warp I by the overall motion before computing ρ_{in} and ρ_{out}.

We need a registration algorithm that is efficient, that can withstand compression artifacts, and that is robust in the presence of multiple motions. The last property is particularly important, since we will often be faced with an image with multiple motions, and our registration algorithm must compute the predominant motion.

We have explored two algorithms, both of which have given satisfactory results. We have experimented with using census transform correlation, a non-parametric approach developed in [10]. This algorithm operates by transforming the image in an outlier-tolerant manner and then using correlation. We have also used the Hausdorff distance [6], an outlier-tolerant method described in Sect. 3.3 that operates on edge-detected images.

It is tempting to exploit the motion vectors contained in MPEG-compressed video in order to determine object or camera motion. Indeed, a number of researchers [11] have attempted to do this. There are a number of reasons that we have not taken this approach. MPEG encoders optimize for compression, and do not necessarily produce accurate motion vectors. MPEG-compressed streams do not contain motion vectors for all images; in fact, if the encoder chooses to create only I-frames, there will be no motion vectors at all.[2]

3 Computing the edge change fraction

Computing the values of ρ for a sequence of images is straightforward. Let δx and δy be the translations necessary to align the images I and I', as calculated by one of the global motion compensation methods discussed in Sect. 2.1. The first step in our algorithm is edge detection.

In our experiments, we have used an edge detector based on Canny's algorithm [3], which thresholds the magnitude of the intensity gradient. Next, copies of E and E' are created with each edge pixel dilated by a radius r. Let us call these dilated images $\bar{E}$ and $\bar{E}'$. Thus, image $\bar{E}$ is a copy of E in which each edge pixel of E is replaced by a diamond whose height and width are $2r+1$ pixels in length.[3] Similarly, image $\bar{E}'$ is a dilated copy of E'.

Consider ρ_{out}, the fraction of edge pixels in E which are farther than r away from an edge pixel in E'. A black pixel $E[x, y]$ is an exiting pixel when $\bar{E}'[x, y]$ is not a black pixel (since the black pixels in $\bar{E}'$ are exactly those pixels within distance r of an edge pixel in E'). The equation for ρ_{out} is

$$\rho_{out} = 1 - \frac{\sum_{x,y} E[x + \delta x, y + \delta y]\bar{E}'[x, y]}{\sum_{x,y} E[x, y]}, \qquad (2)$$

which is the fraction of edge pixels which are exiting. ρ_{in} is calculated similarly

$$\rho_{in} = 1 - \frac{\sum_{x,y} \bar{E}[x + \delta x, y + \delta y]E'[x, y]}{\sum_{x,y} E[x + \delta x, y + \delta y]}. \qquad (3)$$

The edge change fraction ρ shown in Eq. 1 is the maximum of these two values.

The major steps of the computation of the edge change fraction are shown in Fig. 2. The example shows a cut between the two frames. While ρ is being calculated, the locations of the exiting and entering pixels can be saved and their spatial distribution analyzed when looking for wipes and other spatial edits.

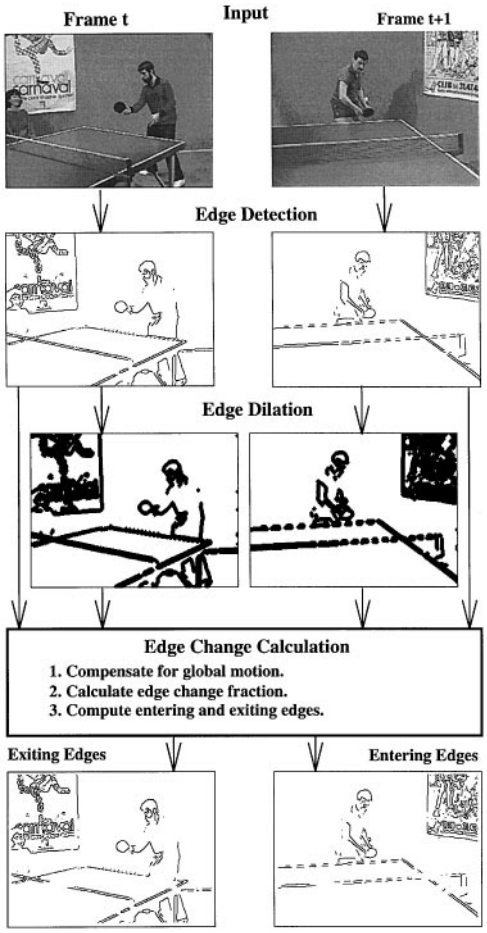

Fig. 2. Main steps of the computation of the edge change fraction

3.1 Peak detection and classification

We propose to detect scene breaks by looking for peaks in the edge change fraction ρ. We have designed a simple

[2] This is not as unusual a situation as one might imagine. About one quarter of the MPEG sequences we have come across on the World-Wide Web are compressed with only I-frames.

[3] To use the Manhattan distance between edges, we dilate by a diamond. If we were to use the Euclidean distance between edges, we would dilate by a circle.

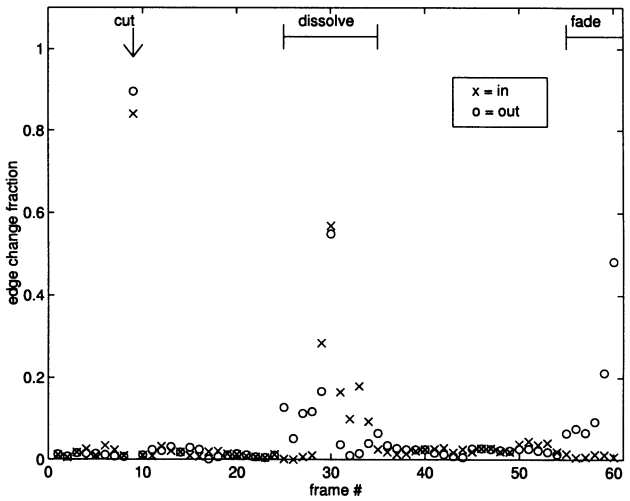

Fig. 3. Values of ρ_{in} (shown as "x") and ρ_{out} (shown as "o") in the table tennis sequence

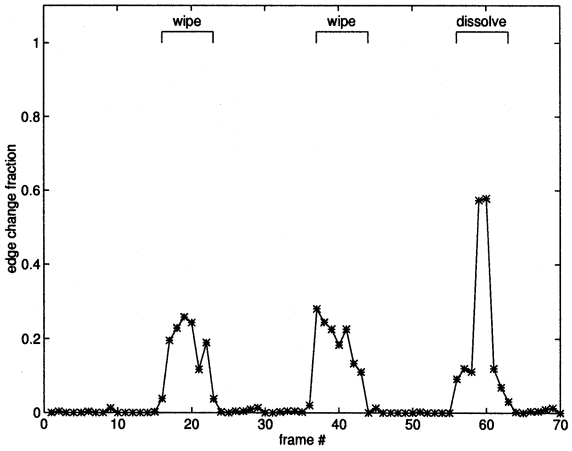

Fig. 4. Results from an image sequence with two wipes and a dissolve

thresholding scheme for peak detection. We use an *event threshold* and an *event horizon*. A frame where ρ exceeds the event threshold may be a scene break. To localize scene breaks that occur over multiple frames, we restrict scene breaks to occur only when ρ is a local maximum within a fixed window of consecutive frames. The width of this window is the event horizon.

3.1.1 Classification

Once a peak has been detected, the next problem is to classify it as a cut, dissolve, fade or wipe. Cuts are easy to distinguish from other scene breaks, because a cut is the only scene break that occurs entirely between two consecutive frames. As a consequence, a cut will lead to a single isolated high value of ρ, while the other scene breaks will lead to an interval where ρ's value is elevated. This allows us to classify cuts.

Fades and dissolves can be distinguished from each other by looking at the relative values of ρ_{in} and ρ_{out} in a local region. During a fade-in, ρ_{in} will be much higher than ρ_{out}, since there will be many entering edge pixels and few exiting edge pixels. Similarly, at a fade-out, ρ_{out} will be higher than ρ_{in}, since there will be many exiting edge pixels, but few entering edge pixels. A dissolve, on the other hand, consists of an overlapping fade-in and fade-out. During the first half of the dissolve, ρ_{in} will be greater, but during the second half ρ_{out} will be greater.

Figure 3 shows the values of both ρ_{in} and ρ_{out} during the table tennis sequence. During the fade-out, ρ_{out} is much higher than ρ_{in}. During the dissolve, there is an initial peak in ρ_{in} followed by a peak in ρ_{out}.

3.1.2 Wipes

Wipes are distinguished from dissolves and fades by looking at the spatial distribution of entering and exiting edge pixels. During a wipe, each frame will have a portion of the old scene and a portion of the new scene. Between adjacent frames, a single strip of the image will change from the old scene to the new scene. For a horizontal wipe there is a vertical strip that passes either left-right or right-left, depending on the direction of the wipe. Since the between-scene transition occurs in this strip, the number of edge pixels that either enter or exit should be higher inside the strip and lower in the other areas of the image. We will call an edge pixel that is either entering or exiting a *changing* pixel.

When computing the edge change fraction, the location of the changing edge pixels can be recorded and their spatial distribution analyzed. There are many ways to analyze the spatial distribution of changing pixels, but we have identified a simple scheme which has yielded good results. We calculate the percentage of such pixels in the top half and the left half of the images, and use this to classify vertical and horizontal wipes. For a left-to-right horizontal wipe, the majority of changing pixels will occur in the left half of the images during the first half of the wipe, then in the right half of the images during the rest of the wipe. Likewise, for a top-to-bottom vertical wipe, the majority of changing pixels will concentrate in the top half, and then in the bottom half. The other two cases (right-to-left and bottom-to-top wipes) can be handled similarly.

Our wipe detection method is aided by the ability of our motion computation to follow the predominant motion. This is particularly important during a wipe, since there can be two rather different motions on the image at the same time. Another aid in discriminating wipes from other scene breaks is that there is no pattern in the values of ρ_{in} and ρ_{out} as there was with dissolves and fades. Also, the relative differences between ρ_{in} and ρ_{out} will be small, since the changing pixels only occur in a limited strip in the image.

Figure 4 shows the edge change fraction in operation on an image sequence containing a left-to-right wipe, a right-to-left wipe, and a dissolve. Figure 5 shows the proportion of the change pixels that occupy the left half of the image (for clarity, this data is only shown when $\rho > 0.05$). Note that, during the left-to-right dissolve, this fraction drops rapidly from 1 to 0, while during the right-to-left dissolve it rises rapidly from 0 to 1. In addition, the pattern during the dissolve is essentially random, as would be expected.

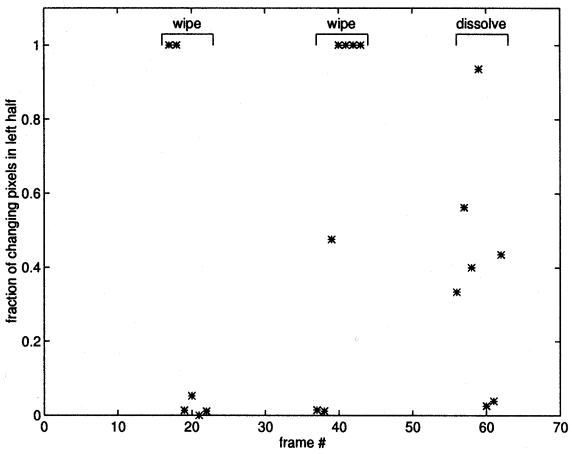

Fig. 5. Spatial distribution of change pixels in an image sequence with two wipes and a dissolve (shown only where $\rho > .05$). Note the random distribution during the dissolve, as compared to the wipes

3.2 Detecting captions

We have extended our work to handle other production effects involving overlays. Many broadcast videos also provide some kind of textual overlay. For example, news broadcasts often begin a story by overlaying the location of the reporter. Similarly, a number of movies and television shows overlay the opening credits on top of a scene.

These textual overlays contain significantly more information than scene breaks, but they share some similarities. Textual overlays can suddenly appear and disappear (like a cut), or gradually fade-in and fade-out (like a dissolve). The pixels in the textual overlay should show up as incoming pixels when they appear, and as outgoing pixels when they disappear.

Examples are shown in Fig. 6. In this sequence, two title captions are overlayed on a "busy" sequence of a waterfall. The first caption is present from the start of the sequence, and then disappears. The second caption appears later. In each case, the caption appears instantaneously (in other words, like a cut rather than like a dissolve). There are significant edges in the background, which causes some degradation in the output. However, the captions clearly show up in the incoming edges. Figure 6 displays, for each caption, the two consecutive images where the caption appears (left sequence) or disappears (right sequence). The figure also show the incoming (left) and outgoing (right) edge pixels.

3.3 The Hausdorff distance

The edge change fraction is related to the Hausdorff distance, which has been used to search for the best match for a model in an image. This distance which has been used for such tasks as recognition and tracking [6]. The Hausdorff distance, which originates in point set topology, is a metric for comparing point sets.

The Hausdorff distance from the point set A to the point set B is defined as

$$h(A, B) = \max_{a \in A} \min_{b \in B} \|a - b\| . \tag{4}$$

Fig. 6. Examples of caption localization

Now consider the Hausdorff distance between the edge-detected images E and E'. If $h(E', E) \leq r$, then every edge pixel in E' is within r of the closest edge pixel in E, there are no entering edge pixels, and so ρ_{in} = 0. Similarly, if $h(E, E') \leq r$, then there are no exiting edge pixels and ρ_{out} = 0.

Most applications of the Hausdorff distance use a generalization called the partial Hausdorff distance, which is

$$h_K(A, B) = K^{th}_{a \in A} \min_{b \in B} \|a - b\| . \tag{5}$$

This selects the K^{th} ranked distance from a point in A to its closest point in B. If we select the largest such distance, we have the original Hausdorff distance defined in Eq. (4).

Applications which use the partial Hausdorff distance for matching [5] can provide a fixed fraction $K/|A|$, which is equal to $1 - \rho$. This specifies what fraction of the points in A should be close to their nearest neighbor in B at the best match. Alternatively, a fixed distance can be supplied, and the fraction of points in A within this distance of their nearest neighbor in B can be minimized. We are using a similar measure as the basis for algorithms to detect scene breaks, which is a very different task than matching.

3.4 Algorithm parameters

Our algorithm has several parameters that control its performance. These parameters include:

- the edge detector's smoothing width σ and threshold τ,
- the expansion distance r,

We have gotten good performance from a single set of parameters across all the image sequences we have tested. These parameters are σ = 1.2 and τ = 24, for the edge

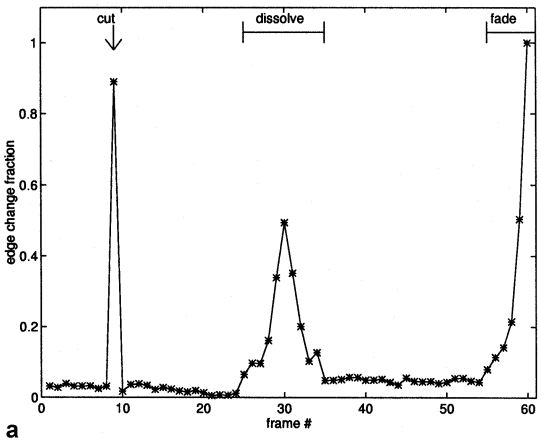

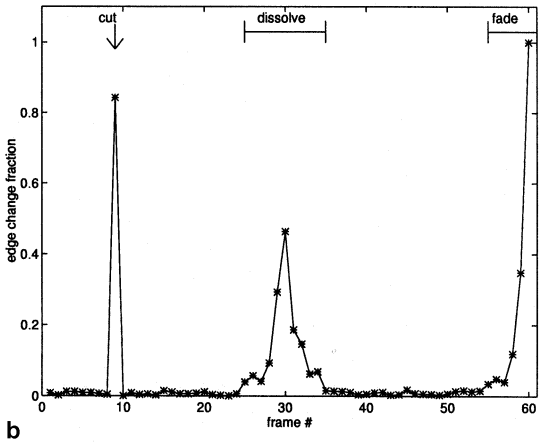

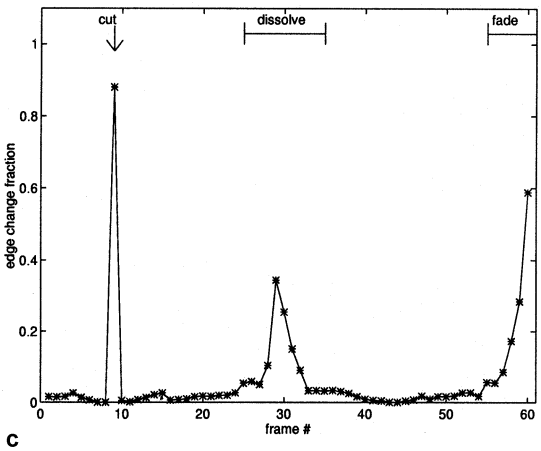

Fig. 7a–c. Results from varying parameters on the table tennis sequence. **a** σ = 1, τ = 32, r = 3; **b** σ = 1, τ = 32, r = 6; **c** σ = 1.8, τ = 12, r = 6

detector, and r = 6. Except where otherwise noted, these were the parameters used to generate the data shown in this paper.

The best choice of parameters, of course, depends upon the image sequence. For example, r should have a very small value for an image sequence with minimal motion, but would have to be large to handle significant independent motion.

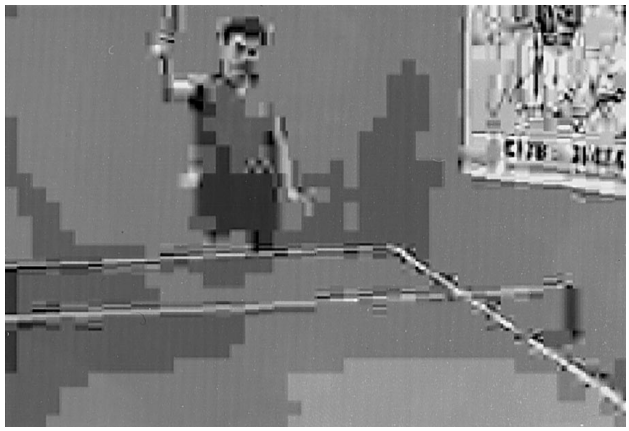

Fig. 8. Table tennis sequence results at 0.18 bits/pixel. Note the significant compression artifacts.

However, we have found empirically that our algorithm's performance is fairly tolerant of different parameter settings. As a demonstration, we have run the table tennis sequence with a variety of different parameters. Figure 7 shows our results with several different values of σ, τ and r.

It is, of course, important that the edge detector parameters are set to obtain a reasonable number of edges. This suggests dynamically thresholding the gradient magnitude, an extension we will discuss in Sect. 5. If r is very small, the algorithm will also perform badly; small shifts in edges (due to noise, non-rigid motion, zooming or compression artifacts) will cause our detector to register false positives. As r gets larger, the value of ρ when there is no scene break decreases, but so does the value during a scene break.

3.5 Compression tolerance

Most video will undergo some form of compression during its existence, and most compression methods are lossy. It is therefore important that our algorithm degrade gracefully in the presence of compression-induced artifacts. While edge detection is affected by lossy compression, especially at high compression ratios, we do not rely on the precise location of edge pixels. We only wish to know if another edge pixel is within r of an edge. As a consequence, the precise location of edge pixels can be changed by image compression without seriously degrading our algorithm's performance. The experimental evidence we present in the next section comes from images that were compressed with the lossy MPEG compression scheme.

To demonstrate the compression tolerance of our approach, we have taken an uncompressed image sequence, added a few scene breaks, and compressed it with a variety of different compression ratios. We have used JPEG compression to benchmark the compression tolerance of our algorithm, because it introduces similar artifacts to MPEG, but is more standardized. (Note that this is only for the data shown in Fig. 8 – the data shown in Sect. 4 came from MPEG-compressed images.)

Figure 8 shows the results from the table tennis sequence when JPEG-compressed to 0.18 bits per pixel (with a quality factor of 3). Our algorithm performed correctly, even though

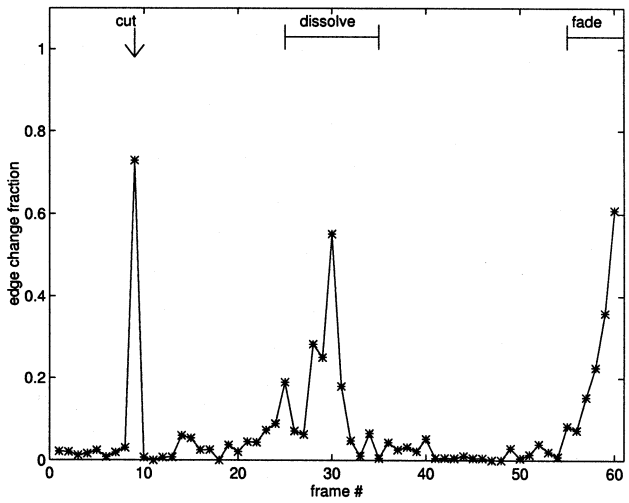

Fig. 9. Table tennis sequence with 4:1 subsampling

the compression artifacts make the sequence almost unviewable. Figure 8 also shows frame #20 at this compression rate.

3.6 Subsampling

Our algorithm also performs well when the input images are subsampled to reduced resolution. Figure 9 shows our algorithm's performance on the table tennis sequence when subjected to 4:1 horizontal and vertical subsampling. Note that the output shown in Fig. 9 is only a little worse than the output that results without subsampling. However, the size of the images is reduced by a factor of 16. Depending on how the registration algorithm is implemented, the speedup can be even greater.

4 Experimental results

We have tested our algorithm on a number of image sequences, containing various scene breaks. To provide a comparison, we have also implemented two other intensity-based measures used to detect scene breaks. The first measure is the intensity histogram difference, which is used with slight variations in most work on scene breaks [7, 8, 11]. The second measure is the chromatic scaling method of Hampapur et al. [4], a recent method for classifying scene breaks.

There are a number of ways to use intensity histograms. Let N denote the number of histogram buckets (which is typically a power of 2 no greater than 256), and let H_t denote the intensity histogram of the t'th frame. The sum of the histogram differences

$$\sum_{i=0}^{N-1} |H_t[i] - H_{t+1}[i]| \tag{6}$$

is one frequently used measure. Another common measure [7] is the χ^2 value

$$\sum_{i=0}^{N-1} \frac{(H_t[i] - H_{t+1}[i])^2}{H_{t+1}[i]} . \tag{7}$$

We implemented a variant of Eq. (6) used by Zhang et al. For each of the three color channels, we used the two most significant bits, for a total of N = 64 bins in the histogram.

4.1 Sources of data

The image sequences used for testing are MPEG movies. We obtained a number of MPEG-encoded movies from `http://www.acm.uiuc.edu/rml/Mpeg/`, which include segments from a number of different sources including music videos, television advertisements, documentaries, and NASA recordings. We selected a number of MPEG movies which contained scene breaks. The running time for our method on these images was around two frames per second, on a single-processor 50-MHz SuperSparc.

In addition, we created some additional MPEG movies. Because the MPEG movies we obtained from the network did not contain enough scene breaks to generate significant data, we spliced together scenes from existing MPEG movies and inserted a variety of scene breaks. These spliced movies have several advantages: they show many different scene breaks at known locations, but the video itself was shot and compressed by third parties. Finally, we created one movie, called `andy`, from video which we shot. We inserted several scene breaks during the editing process, and then compressed it using the Berkeley MPEG encoder.

The data we used is highly compressed. The following table summarizes the compression parameters of several of the image sequences we used.

Sequence	Bits per pixel	Dimensions
`clapton`	0.91	160×120
`spacewalk`	0.82	160×120
`andy`	0.35	160×112

All these sequences are color, so the compression ratios (from 24-bit color images) range from 26:1 to 69:1. These high compression ratios probably result from using videos available on the World-Wide Web, which places a premium on compression to minimize bandwidth and storage costs. However, this makes our data set representative of the kind of video that is widely available today.

All of the test sequences shown use the parameter values mentioned above. The chromatic scaling method and the histogram difference, which we show for comparison, involve no parameters. All of these methods are intended to produce distinctive peaks at cuts and dissolves.

4.2 Comparative results on difficult sequences

The image sequences we have collected fall into three classes. Several image sequences had easy scene breaks, which could be detected by all the methods we tried. For example, there may only be cuts, or there may be minimal motion. Another class of image sequences caused errors for conventional intensity-based methods, but were handled correctly by our feature-based method. Examples include sequences with motion, and especially ones with both motion and dissolves. Finally, certain image sequences yielded incorrect answers, no matter what method we used. Examples

include commercials with very rapid changes in lighting and with fast-moving objects passing right in front of the camera.

In our discussion, we will concentrate on sequences where some algorithm had difficulty detecting the scene breaks. On the 50 MPEG movies we examined, we did not find an example where our method failed but where intensity-based methods worked.

4.2.1 The Clapton sequence

One MPEG video that we obtained is part of an Eric Clapton music video. It is an interesting sequence because it contains two dissolves, as well as a moving object (the singer). It has been used to benchmark other algorithms (e.g., [4]). Figure 10 shows the performance of several measures on this sequence. The edge change fraction detects and classifies both dissolves correctly. The image from each dissolve with the highest value of ρ is shown in Fig. 13 (these are the images that are at the center of the two dissolves according to our detection method described in Sect. 3.1).

The intensity histogram difference, shown in Fig. 10b, is a noisier measure on this sequence. It does show a rise during the first dissolve, and it is possible that the dual threshold scheme of [11] would detect this (depending on the exact thresholds used). However, the second dissolve appears to be indistinguishable from the noise. Their method for handling motion would not help here, since the problem is a false-negative rather than a false-positive.

The chromatic scaling feature of [4] is shown in Fig. 10c. As the authors state, their method has difficulty with dissolves involving motion.

From these results it is not clear whether the histogramming method would find the first dissolve. Depending on how the data is thresholded, either the second cut would be missed or a false cut would be detected at frames #137–#138. These two frames are shown in Fig. 14.

4.2.2 The Andy sequence

Another sequence that caused some difficulty is the andy MPEG. The sequence involves camera and object motion, as well as zooms. It was the most highly compressed MPEG movie that we examined and consists of five scenes separated by three cuts and one dissolve. Frames #1–#50 consist of a stationary scene with the camera panning from right to left. The sequence then cuts to a scene in frames #51–#99 during which the camera zooms in on a stationary background. There is another cut to a scene in frames #100–#133 consisting of a zoom out from a stationary background. The camera stops zooming and continues on the same stationary background for frames #133–#170 and camera remains still on the stationary background. Following the third cut, the sequence contains a scene with a moving person walking from left to right with the camera panning to the right to follow the individual during frames #171–#230. Frames #231–#240 consist of a dissolve between this scene and another in which the camera pans to the right with a stationary background.

Figure 11 presents the results of our method and the intensity histogram difference. The image from the dissolve with the highest value of ρ (frame #235) is shown in Fig. 12. While we have run the chromatic scaling method on andy, it does not produce good results because the sequence includes so much motion.

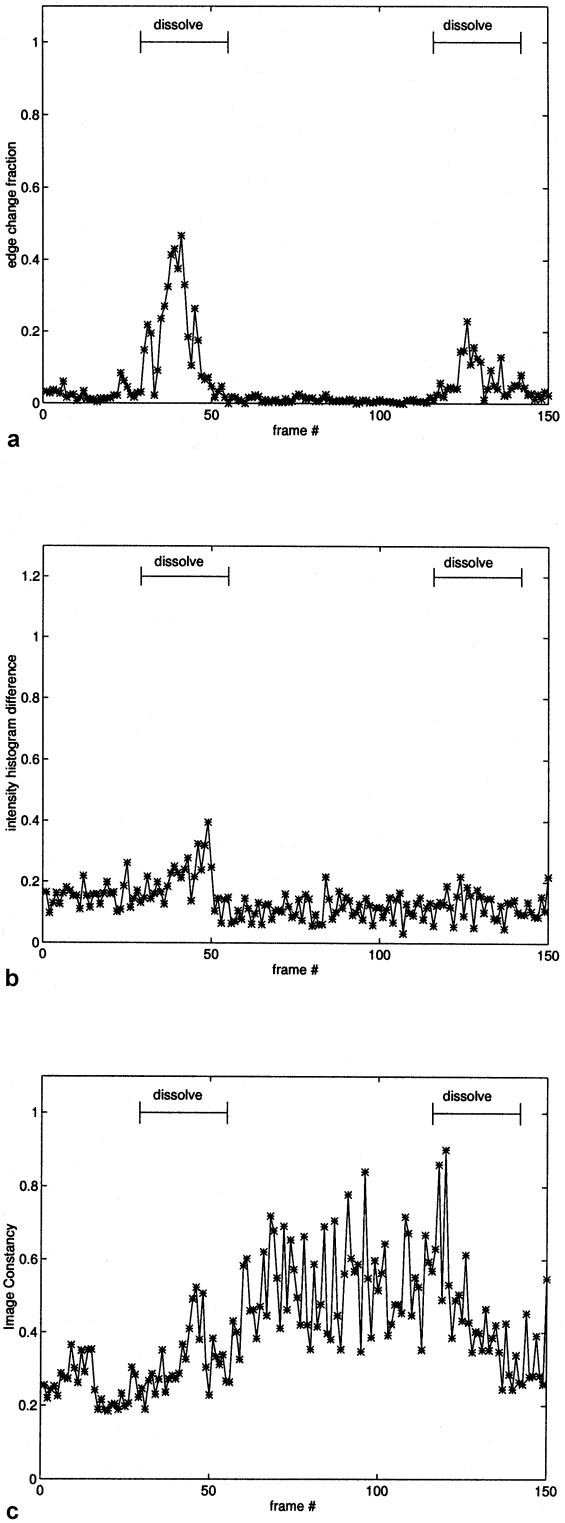

Fig. 10a–c. Results from the Clapton sequence. **a** Edge change fraction; **b** intensity histogram difference; **c** chromatic scaling feature

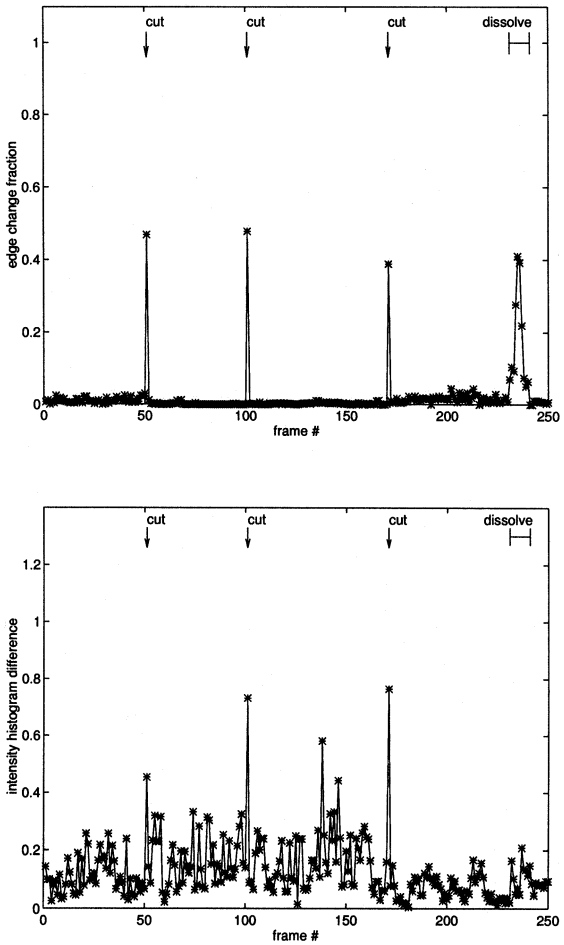

Fig. 11a,b. Results from the andy sequence. **a** Edge change fraction; **b** intensity histogram difference

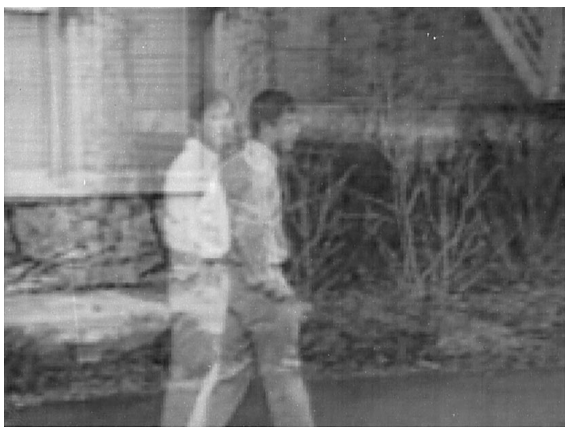

Fig. 12. Image from andy sequence detected as dissolve by our method

4.3 Availability

Code for running the algorithm is available via FTP from the host ftp.cs.cornell.edu in the directory /pub/dissolve. The code and the image sequences we used can be found starting from the first author's home page on www.cs.cornell.edu/home/rdz.

Fig. 13. Images from clapton sequence detected as dissolves by our method

5 Limitations and extensions

Our algorithm's failures involve false negatives, and result from two limitations in our current method. First, the edge detection method does not handle rapid changes in overall scene brightness, or scenes which are very dark or very bright. Second, our motion compensation technique does not handle multiple rapidly moving objects particularly well.

The edge detection used in our algorithm has a few limitations at present. For example, rapid changes in overall scene brightness can cause a false positive. Since a thresholded gradient-based edge detector is dependent on the relative contrast of regions in the image, large-scale scalings in image brightness will disturb the edge density of the scene. This effect sometimes occurs in scenes due to camera autogain.

Scene break detectors based on intensity histogramming will also generate false positives when the overall scene brightness changes dramatically. Although the intensities change dramatically, the underlying edge structure of the image does not change. A more robust edge detection scheme may enable us to handle these events.

Another improvement, also discussed in [11], involves handling multiple moving objects. The clapton sequence contains some motion, while the andy sequence contains significant motion (both camera and object motion). As the above data shows, our algorithm handles these sequences well. However, the algorithm's handling of multiple moving objects could probably be improved by compensating for multiple motions.

A number of algorithms have been proposed for this problem in the computer vision literature. When there are two distinct motions in the scene, our motion compensation

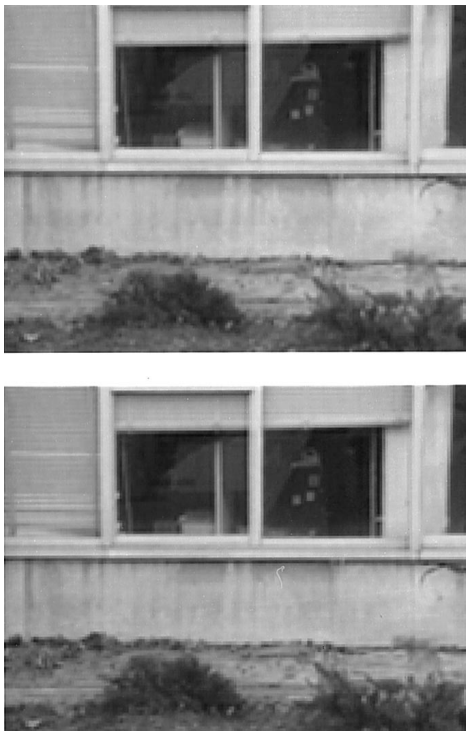

Fig. 14. Consecutive images from andy sequence with large intensity histogram difference

will track one of them. Edges that undergo the other motion will show up as entering or exiting pixels, assuming that the two motions are sufficiently distinct. We may be able to use these changing pixels to identify objects undergoing a different motion. A solution to this problem would allow users to search a video for the next entrance of an additional moving object.

Another interesting extension involves combining our feature-based algorithm with an intensity-based approach. For example, a conservative intensity-based scheme might be designed which can reliably determine that there are no scene breaks in some portion of a video. Our algorithm might be invoked when the intensity-based scheme indicates a potential scene break. Such a hybrid scheme could be much faster than our method, especially if the intensity-based component operated directly on compressed data.

Since the methods we use are fundamentally non-linear, it seems unlikely that we will be able to operate directly on compressed data streams without decompressing. However, our scheme is reasonably fast, and can be optimized further. Our method also appears to give good results on reduced-resolution imagery, as shown in Fig. 9. Finally, much of the overhead of MPEG decompression is due to dithering (for example [9] states that dithering consumed 60–80% of the time in their MPEG decoder). Since our approach only uses intensity information, this phase of MPEG decompression can be bypassed.

Conclusions

We have described a new approach to detecting and classifying scene breaks. Our methods robustly tolerate motion, as well as compression artifacts. We are incorporating our algorithm into a browser for MPEG videos which allows the user to search for scene breaks. In the future, we hope to be able to add higher level search capabilities to this browser.

Acknowledgements. This research has been supported by DARPA under contract DAAL01-97-K-0104, monitored by ONR. We are grateful to the anonymous reviewers, and to Dan Huttenlocher and Brian Smith, for suggestions that improved the presentation of this material.

References

1. Boreczky JS, Rowe LA (1996) A comparison of video shot boundary detection techniques. J Electronic Imaging 5(2):122–128. Also appears in SPIE Proceedings number 2670
2. Brown L (1992) A survey of image registration techniques. ACM Comput Surv 24(4):325–376
3. Canny J (1986) A computational approach to edge detection. IEEE Trans Pattern Anal Mach Intell 8(6):679–698
4. Hampapur A, Jain R, Weymouth T (1995) Production model based digital video segmentation. J Multimedia Tools Appl 1:1–38
5. Huttenlocher D, Jaquith E (1995) Computing visual correspondence: Incorporating the probability of a false match. In: 5th International Conference on Computer Vision, pp 515–522
6. Huttenlocher D, Klanderman G, Rucklidge W (1993) Comparing images using the Hausdorff distance. IEEE Trans Pattern Anal Mach Intell 15(9):850–863
7. Nagasaka A, Tanaka Y (1991) Automatic video indexing and full-video search for object appearances. In: 2nd Working Conference on Visual Database Systems
8. Otsuji K, Tonomura Y (1994) Projection-detecting filter for video cut detection. Multimedia Systems 1:205–210
9. Rowe LA, Patel K, Smith BC (1993) Performance of a software MPEG video decoder. In: ACM Multimedia Conference
10. Zabih R, Woodfill J (1994) Non-parametric local transforms for computing visual correspondence. In: 3rd European Conference on Computer Vision, pp 151–158
11. Zhang HJ, Kankanhalli A, Smoliar SW (1993) Automatic partitioning of full-motion video. Multimedia Systems 1:10–28

RAMIN ZABIH is an assistant professor of Computer Science at Cornell University. He received undergraduate degrees in Computer Science and Mathematics, and a master's degree in Computer Science, from MIT. His PhD was awarded by Stanford in 1994. His research interests are in computer vision and its applications. He has served on the program committees of conferences in both multimedia and computer vision.

JUSTIN MILLER received his BS and MEng degrees in computer science from Cornell University in 1995 and 1996, respectively. He is currently serving as a nuclear submarine officer in the US Navy. His research interests include image feature extraction, motion analysis, user interface design and fast feature-based search algorithms for image databases.

KEVIN MAI received a B.S. in computer science from Cornell in 1995, and an M. Eng in 1996. He is currently out in the workforce.